Intercepting a Transient Pyridine N-Oxide Fe(III) Species in Catalytic Oxygen Atom Transfer Reaction

Nhat Tam Vo, Christian Herrero, Régis Guillot, Tanya Inceoglu, Winfried Leibl, Martin Clémancey, Patrick Dubourdeaux, Geneviève Blondin, Ally Aukauloo, Marie Sircoglou

▶ **To cite this version:**

Nhat Tam Vo, Christian Herrero, Régis Guillot, Tanya Inceoglu, Winfried Leibl, et al.. Intercepting a Transient Pyridine N-Oxide Fe(III) Species in Catalytic Oxygen Atom Transfer Reaction. Chemical Communications, 2021, 57 (95), pp.12836-12839. 10.1039/D1CC04521K . hal-03678000

HAL Id: hal-03678000
https://hal.science/hal-03678000

Submitted on 25 May 2022

HAL is a multi-disciplinary open access archive for the deposit and dissemination of scientific research documents, whether they are published or not. The documents may come from teaching and research institutions in France or abroad, or from public or private research centers.

L'archive ouverte pluridisciplinaire **HAL**, est destinée au dépôt et à la diffusion de documents scientifiques de niveau recherche, publiés ou non, émanant des établissements d'enseignement et de recherche français ou étrangers, des laboratoires publics ou privés.

COMMUNICATION

Intercepting a Transient Pyridine N-Oxide Fe(III) Species in Catalytic Oxygen Atom Transfer Reaction

Received 00th January 20xx,
Accepted 00th January 20xx

DOI: 10.1039/x0xx00000x

Nhat Tam Vo,[a] Christian Herrero,[a] Régis Guillot,[a] Tanya Inceoglu,[a] Winfried Leibl,[b] Martin Clémancey,[c] Patrick Dubourdeaux,[c] Geneviève Blondin,[c] Ally Aukauloo*[a,b] and Marie Sircoglou*[a]

In the context of bioinspired OAT catalysis, we developed a tetradentate dipyrrinpyridine ligand, halfway between hemic and non-hemic models. The catalytic activity of the iron(III) derivative was investigated in presence of iodosylbenzene. Unexpectedly, MS, EPR, Mössbauer, UV-Visible and FTIR spectroscopic signatures supported by DFT calculation provide convincing evidence for the reversible formation of a relevant Fe^{III}-O-N_{Py} intermediate.

Oxygen Atom Transfer (OAT) reactions are important in chemical synthesis and biology where high valent metal-oxos are key catalytic species.[1] Bioinspired models have been investigated to replicate the reactivity and selectivity of hemic and non-hemic enzymes. After much effort, chemists have unravelled facets of the structure and function relationship of the catalytic intermediates that affect substrate oxidation.[2] While the reactivity studies have long been focused on +IV and +V oxidation state metal-oxo intermediates, multiple active oxidant mechanisms have also been proposed (Scheme 1).[1a,3] For instance, iron(III) iodosylarene adducts have been considered as alternate active species.[4] In-depth studies, implying chemical variation of the iodosylarene,[5] X-ray structure characterization of such intermediate[6] and DFT calculations[7] have contributed to support this pathway. In parallel, pyridine N-oxides have been used as terminal oxidant in molecular metal complexes assisted OAT reactions.[8] Che and coll. have in particular reported interesting OAT activities of a wide variety of organic substrates by combining ortho-substituted pyridine N-oxide with Ru catalysts.[9] Fukuzumi and coll. also demonstrated the photoactivation of an embarked outer sphere pyridine N-oxide fragment in a ruthenium-based complex to transfer the oxygen atom to an organic substrate.[10] More generally, the propensity to use heteroarene N-oxides as oxygen source in organic reactions was recently highlighted by Pospech. In this review, no mention is made of inner-sphere bound pyridine N-oxide as potential catalytic species towards OAT reactions.[11] Yet, in several investigations, iron-N-oxide species have been characterized. McKenzie and coll. reported the chemical alteration of an Fe(V)-oxo species in the form a metal bonded tertiary amine N-oxide that was characterized crystallographically.[12] In another example, the flexibility of a hexadentate ligand was proposed to favour the stabilization of an electrophilic oxyl group by a pendant pyridyl arm.[6] More recently the lack of reactivity of a putative $[LFeO]^{2+}$ intermediate was attributed to the formation of pyridine N-oxide iron(III) complex, devoid of any catalytic activity.[13] Henceforth, in the actual state of the art, there is no report of any case where post synthetic iron N-oxide species can themselves be involved in a catalytic OAT reaction to organic substrates. On the contrary, their formation is rather considered as deleterious pathway.

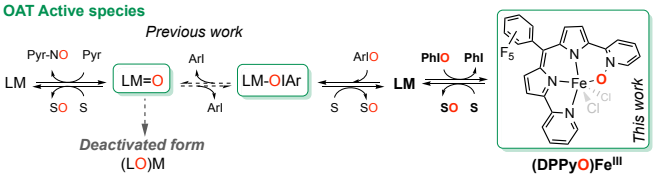

Scheme 1. Generation of relevant species involved in OAT reactions with iodosylarene and and pyridine N-oxide oxidants.

In this study, we report the synthesis of an iron(III) complex supported by a semi-hemic dipyrrinpyridine ligand, shorthanded as DPPy under its deprotonated form. The design of the ligand was directed to exclude alkyl chains in the backbone to limit its flexibility and increase its robustness towards self-oxidation.[14] We found that in presence of iodosylbenzene, $[Fe^{III}DPPyCl_2]$ could promote the oxidation of a fair variety of substrates. In the process to unravel the nature of the putative oxidizing reactive species, no spectroscopic signatures for a highly oxidized Fe-oxo intermediate were detected. However, MS and IR collected data provide concurring evidence for the chemical formulation of an $[Fe^{III}(DPPyO)Cl_2]$ intermediate. EPR and Mössbauer spectroscopy also nails the formation of a high spin Fe(III)

[a] ICMMO, Université Paris Saclay, CNRS, F-91405 Orsay Cedex, France.
[b] Institute for integrative Biology of the Cell (I2BC), CEA, CNRS Université Paris-Saclay, UMR 9198, F-91191, Gif-sur-Yvette, France.
[c] Laboratoire de Chimie et Biologie des Métaux, Univ. Grenoble Alpes, CNRS, CEA, IRIG, 17 rue des Martyrs, F-38000 Grenoble, France.
Electronic Supplementary Information (ESI) available. See DOI: 10.1039/x0xx00000x

Please do not adjust margins

transient species. These intrigues are elucidated in what follows with the support of DFT calculations.

The DPPyH ligand and the [Fe^{III}DPPyCl$_2$] complex were prepared by adapting reported procedures (see ESI). Dark blue single crystals of the complex were obtained from an Et_2O/ACN mixture. The molecular structure was determined by X-ray diffraction (XRD) analysis (Fig. 1). The coordination sphere around the iron ion is a distorted octahedron with four nitrogen atoms in a plane and two pseudo-axial chloride ligands held at an angle of 152° from the metal. The open structure of the DPPy ligand leads to a trapezoidal N4 coordinating scheme supported by two short metal-ligand bond with the dipyrrin pointing at Fe-N_1 and Fe-N_2 = 2.048(3) Å and two longer ones involving the pyridine rings (Fe-N_3 and Fe-N_4 = 2.238(4) Å). These bond lengths are respectively equivalent to those of Fe(III) porphyrin complexes (av. 2.02 Å) and longer than those encountered classically in pyridine containing ligands (av. 2.15 Å, see ESI). The XRD analysis of crystals grown in acetone indicated two different conformations, one where the DPPy backbone is severely twisted by 14.70° while the second exhibits a dissymmetric coordination pattern (See ESI and Fig. S1-S4). These structural snapshots point to a certain displacement of the iron(III) to adapt within the trapezoidal coordinating N4 pattern supported by the DPPy ligand. The consequence of this, results in the distancing of the iron ion away from one of the pyridine group as schematized in Fig. 1.

The X-band EPR spectrum of the complex was recorded at 10 K in acetonitrile and revealed three signals with g values at 9.1, 5.1 and 3.7 consistent with high spin (S = 5/2) Fe(III) species (Fig. S6). This spectrum was best simulated with the contribution of two high spin species probably originating from subtle structural difference as observed in the solid state.

The catalytic activity of [FeDPPyCl$_2$] was evaluated in the presence of iodosylbenzene as an oxygen atom donor. Under unoptimized conditions, quantitative oxidation of triphenylphosphine and thioanisole were observed at room temperature. More challenging substrates such as cyclooctene, toluene or cyclohexane, were also oxidized with good to modest yields (Scheme 2, Table S3). The observed reactivity matches those reported for hemic and non-hemic OAT catalysts, prompting us to further investigate the nature of the catalytic species involved in this unique hybrid hemic/non-hemic system.

Our first experiment consisted in the monitoring of the electronic absorption spectral features of a solution of complex [FeDPPyCl$_2$] in acetonitrile upon addition of a stoichiometric amount of PhIO at room temperature. The starting iron(III) complex presents two strong absorption bands in the region spanning from 500 to 700 nm. Such features are also present

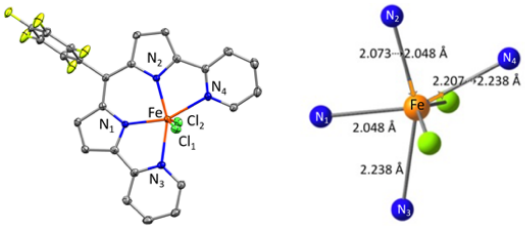

Fig. 1 *Left*: ORTEP view of the XRD structure of [FeDPPyCl$_2$], single crystals grown in Et_2O/ACN, H omitted, ellipsoids at 30%; *Right*: Scheme showing Fe displacement in the N_4 cavity upon changing the solvent of crystallization to acetone.

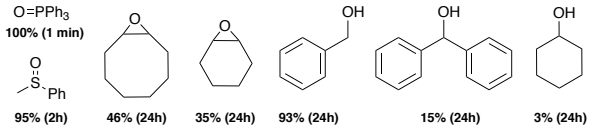

Scheme 2. Main oxidation products obtained upon catalytic oxidation by [FeDPPyCl$_2$] with PhIO (20 eq.) in acetonitrile. Conversions determined by GC.

for the free ligand albeit with different amplitudes and energies.[15] Accordingly, the absorption bands for the [FeDPPyCl$_2$] complex are likely attributed to metal-ligand and/or ligand-ligand charge transfer bands. As depicted in Fig. 2, addition of PhIO caused the instant bleach of the precursor band at 650 nm and apparition of a strong absorption band at 636 nm ($\varepsilon \approx 20\,000$ L mol^{-1} cm^{-1}) with a concomitant drop in intensity of the initial absorption band at 589 nm (ε = 21 600 L mol^{-1} cm^{-1}). Coincidentally, weaker absorption bands have been reported for non-hemic iron-oxo intermediates in this spectral window although with lower ε values to confound with the actual bands.[16] This new prominent spectral feature then faded away within 15 mins to rest the initial UV-vis spectrum of [FeDPPyCl$_2$] (λ_{max} = 589 nm, ε = 21 600 L mol^{-1} cm^{-1}) albeit with slightly different relative intensities. Such an evolution can be related to the generation of an active species that would react with the solvent to regenerate the starting complex. During this process, some modification of the coordination sphere of iron may occur, explaining the slight difference observed in the recovered absorption spectrum. In another experiment, when triphenylphosphine was added to the oxidized species, the decay was accelerated by a factor of 5 (3 mins) while triphenylphosphine oxide was detected by Mass spectroscopy (MS) and NMR. This result put us on track that the monitored intermediate, denoted as species **I** is a relevant OAT agent.

We then interrogated the oxidation state of this intermediate using X-band EPR spectroscopy. As can be seen in Fig. 2, the initial signal of the precursor [FeDPPyCl$_2$] complex was replaced by a broad rhombic signal at g = 4.28 (E/D = 0.33) with an estimated conversion of around 60%. In addition, no signal was detected in parallel mode most probably precluding an integer spin state for the reactive intermediate. Besides no Fe-oxo intermediate could be detected even upon reaction at lower temperature. Unequivocally, addition of triphenylphosphine conducted to the disappearance of the signal at 4.28 with the concurrent recovery of the initial EPR signals of the precursor. These results therefore suggest that the reactive species **I** contains a high spin Fe(III) ion in a rhombic environment. Further confirmation for the oxidation state of **I** comes from the

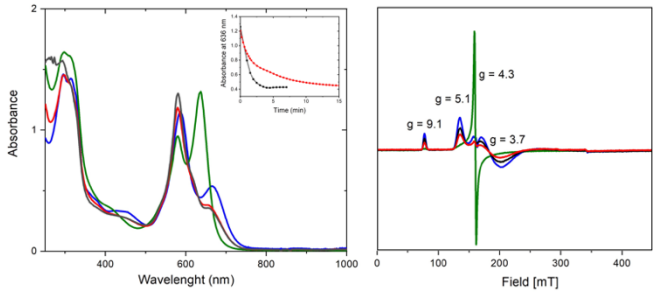

Fig. 2 Spectral changes of a [FeDPPyCl$_2$] solution in ACN before (blue) and after (green) oxidation by PhIO, followed by its degradation (red) or reaction with PPh_3 (black). Left: UV-vis, Inset: degradation kinetics; Right: X-band EPR at T=10K.

This journal is © The Royal Society of Chemistry 20xx

Please do not adjust margins

Please do not adjust margins

Mössbauer analysis of a ^{57}Fe enriched intermediate **I** at 6K (Fig. S8). Upon addition of PhIO, the broad dissymmetric doublet, (δ = 0.45 mm s^{-1}, ΔE_Q = 0.78 mm s^{-1}) of the starting complex gives rise to a new spectrum that can be described as the main contribution of a broad sextet extending from – 8 to 9 mm s^{-1} (64%, δ = 0.46 mm s^{-1}, ΔE_Q = 0.61 mm s^{-1}) attributed to the signature of a S=5/2 species and a quadrupolar doublet (39%, δ = 0.51 mm s^{-1}, ΔE_Q = 1.59 mm s^{-1}) most probably arising from a magnetically silent μ-oxo dimeric species generated under the high concentration of the Mössbauer analysis.[17] No genuine Fe(V) or Fe(IV)=O signatures were identified therefore ruling out such formulation for the transient species previously detected by UV and EPR.

Interestingly, upon ageing of the previous solution, the main magnetic Mössbauer signal disappeared to give a 1:1 mixture of the starting signal and the diamagnetic doublet (Fig. S8 bottom). These results again provide support for the formation of an Fe(III) transient species, **I**.

At this juncture, we cogitated on a first alternative for the description of an iron(III) species that can behave as an oxygenated atom source. For this, we turned our attention to the formation of a Fe(III) iodosylbenzene adduct that has already been reported in literature by Nam and McKenzie. Mass spectrometry analysis is extremely sensitive and can permit the detection of unexpected highly active intermediates or chemically altered forms of the catalyst upon reaction with the chemical oxidant for instance. A solution of [FeDPPyCl$_2$] in acetonitrile was treated with PhIO and followed by High Resolution ESI-MS. A peak of weak intensity was detected at 773.9389 that corresponds to the iodosylbenzene adduct. However, several more prominent peaks were also present. Although the relative intensities of the mass-to-charge ratio do not necessarily reflect the actual concentration of the species in solution, we were piqued to investigate the nature of these signals. First, we identified a peak pointing at 534.0194 that matches the formula [FeDPPy(O)–H]$^+$ and can tentatively be assigned to a C-H hydroxylation product (see ESI). Such hydroxylation of aromatic rings has been observed in prior studies[18] and might partially account for the incomplete recovery of the initial absorption spectrum described above. Two peaks of interest were also evidenced at 569.9954 and 580.0242 that corresponds to the chemical formulations [FeDPPy(O)Cl]$^+$ and [FeDPPy(O)(HCOO)]$^+$ respectively (Fig. S9). These peaks were sensitive when labelled $H_2{}^{18}O$ was added after reaction with PhIO. This result supports the fact that the transferred oxygen atom is chemically labile towards exchange within these species (Fig. S10). Having previously ruled out the formation of iron oxo species, an additional signal peaking at 503.0879 caught our attention. This peak relates to a molecular fragment [(DPPyH(O)+Na]$^+$, i.e. the sodium adduct of the free ligand with an inserted oxygen atom.[19] With this formulation, a reasonable site for such a reaction is one of the pyridine groups to form an N-O pyridine noted as (DPPyO). Such oxygen insertion into a metal-heteroatom bond have been well documented with pyridine-amines containing ligands.[20] In our case, the rigid conjugated acyclic skeleton of the DPPy ligand resulting in a loose coordination of the iron(III) ion is probably the crucial structural factor that facilitates the oxygen insertion to form a [Fe^{III}(DPPyO)Cl$_2$] species. Similar oxygen atom insertion was attested crystallographically by Lau and coll. with an analogous quarterpyridine ligand to form a quaterpyridine-dioxide ruthenium complex acting as the active species for the water oxidation reaction.[20b] In our case, all attempts to crystallize such an intermediate failed due to its short life time and its high solubility. However, infrared spectroscopy provided supportive evidence for the presence of the N-O bound fragment. Compared to the initial [FeDPPyCl$_2$] complex, two new bands sensitive to ^{18}O labelling were clearly apparent at 1226 and 845 cm^{-1} on the IR spectrum of a [FeDPPyCl$_2$] / PhIO mixture (Fig. 3 and S12). These two signals can be respectively assigned to the stretching and bending vibration mode of the pyridine N-O$_{Fe}$ bond by comparison to the values reported for Fe(OPy)$_6$(ClO$_4$)$_3$ (1214, 839 cm^{-1}).[21] Importantly, these bands were absent in aged solutions and can therefore be related to a transient species.

With a systematic approach to analyze the reactivity pattern with other terminal oxidants, we assessed the reactivity with *m*CPBA and NaClO. In the presence of *m*CPBA, a rapid degradation of the precursor was observed. However, when NaClO was used instead of PhIO, very similar spectra were obtained by UV-Vis, EPR, MS and IR spectroscopy (Fig. S13-S16). As with PhIO, the new spectral features were bleached upon addition of triphenylphosphine (Fig. S14). These collected results bring additional support for the formation of a potent reactive [Fe^{III}(DPPyO)Cl$_2$] intermediate in OAT reactions.

Based on these original finding in the OAT reactions, we were interested to rationalize our observations with the support of DFT calculations. In a first place, our DFT study indicates an activation energy of 7.9 kcal.mol^{-1} for the decoordination of one of the pyridine ligand, thus suggesting some equilibrium might occur in solution at room temperature (see ESI). Then, we investigated the structure of intermediate **I**. The most stable geometry located features the insertion of an oxygen atom in one of the Fe-N$_{py}$ bonds (Fig. 3 and ESI). The iron center and the 3 unaffected nitrogen atoms hardly deviate from their initial positions (Fig. S20). While, the ClFeCl angle flattens compared to the computed precursor (156 to 143°) and the pyridine N-oxide ring tilts by 27° from the N4 plane to allow the bent N-O-Fe connection to form (Fe-O = 2.09 Å, N-O = 1.32 Å, NOFe = 123°). Vibrational analysis of the computed [Fe^{III}DPPy(O)Cl$_2$] revealed two modes involving N-O stretching and bending at 1233 and 852 cm^{-1}. As observed experimentally these

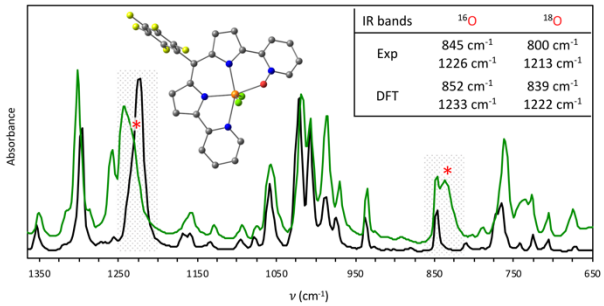

Fig. 3 FTIR spectra of [FeDPPyCl$_2$] before (black) and after (green) addition of PhIO; Inset: computed [Fe(DPPyO)Cl$_2$] structure, Table: Experimental isotope sensitive bands compared to the calculated vibration modes involving N-O bonds

Please do not adjust margins

Please do not adjust margins

frequencies were isotopically shifted to higher energies (Fig. 3, S18-19), thus comforting our hypothesis. Although a full study of the mechanistic pathway leading to the formation of the pyridine N-oxide adduct is beyond the scope of this paper, we theoretically investigated the putative iron(V)-oxo and iron(III)-iodosylbenzene intermediates (Fig. S21). By contrast, these notional structures were respectively found 35 and 21 kcal mol^{-1} less stable than the computed [Fe^{III}(DPPyO)Cl_2], indicating that such species if they are formed, should alter rapidly. Of particular relevance, we noticed the departure of one pyridine arm in the Fe-oxo adduct. As stated above, the DPPy ligand probably provides a somewhat rigid N4 coordinating cavity and therefore cannot flex enough to accommodate the smaller highly oxidized iron(IV) or iron(V) ion. Such a structural feature in the designed DPPy ligand agrees with a possible intramolecular OAT to the free pyridine.

In this study, we have investigated the OAT reactivity of a newly developed iron(III)-dipyrrin-dipyridine complex, [Fe^{III}DPPyCl_2]. UV-vis, Mössbauer and EPR spectroscopies point to the formation of an Fe(III) active species, while ESI-MS and IR and analysis corroborated by DFT helped us identifying the oxygenation of a Fe-N_{py} bond. Oxygen insertion in ligand-Fe bonds has only been observed in rare cases and were most often considered as dead ends devoid of any reactivity.[13,22] Herein, upon treatment of [Fe^{III}DPPyCl_2] with an oxygen-containing oxidant such as PhIO, we propose the formation of intramolecular Fe^{III}-O-N_{Py} intermediate that still allows O-delivery to various organic substrates. Such a behavior has to our knowledge only been observed in the case of Ru complexes and under light irradiation.[10] Whether the mechanism involving the [Fe^{III}(DPPyO)Cl_2] intermediate **I** for the O-atom delivery to organic substrates proceeds via the classic generation of a potent Fe=O or a concerted pathway still remain to be elucidated. Future modifications of the DPPy backbone will help us to decipher and optimize the unusual oxidation process reported herein.[23] Work along these lines is in progress.

We thank ANR-15-CE07-0021-01, ANR-17-EURE-0003, LabEx CHARM³AT & ARCANE, HPC resources (GENCI-A0070810977), DataCenter@UPSud. GB thanks Dr V.Maurel for EPR recordings.

Notes and references

1 a) J.T. Groves, R.C. Haushalter, M. Nakamura, T.E. Nemo, B.J. Evans, *J. Am. Chem. Soc.*, 1981, **103**, 2884; b) A.R. McDonald, L. Que, Jr., *Coord. Chem. Rev.*, 2013, **257**, 414; c) J. Chen, A. Draksharapu, D. Angelone, D. Unjaroen, S.K. Padamati, R. Hage, M. Swart, C. Duboc, W.R. Browne, *ACS Catal.*, 2018, **8**, 9665; d) M. Guo, T. Corona, K. Ray, W. Nam, *ACS Cent. Sci.*, 2019, **5**, 13.

2 a) D. Usharani, D. Janardanan, C. Li, S. Shaik, *Acc. Chem. Res.*, 2013, **46**, 471; b) W. Nam, Y.-M. Lee, S. Fukuzumi, *Acc. Chem. Res.*, 2014, **47**, 1146; c) W.N. Oloo, L. Que, *Acc. Chem. Res.*, 2015, **48**, 2612.

3 a) J.T. Groves, T.E. Nemo, R.S. Myers, *J. Am. Chem. Soc.*, 1979, **101**, 1032; b) Y. Yang, F. Diederich, J.S. Valentine, *J. Am. Chem. Soc.*, 1990, **112**, 7826; c) K. Machii, Y. Watanabe, I. Morishima, *J. Am. Chem. Soc.*, 1995, **117**, 6691.

4 a) J.P. Collman, A.S. Chien, T.A. Eberspacher, J.I. Brauman, *J. Am. Chem. Soc.*, 2000, **122**, 11098; b) M. Guo, Y.-M. Lee, S. Fukuzumi, W. Nam, *Coord. Chem. Rev.*, 2021, **435**, 213807.

5 a) W. Nam, S.K. Choi, M.H. Lim, J.-U. Rohde, I. Kim, J. Kim, C. Kim, L. Que, Jr., *Angew. Chem. Int. Ed.*, 2003, **42**, 109; b) S. Hong, B. Wang, M.S. Seo, Y.-M. Lee, M.J. Kim, H.R. Kim, T. Ogura, R. Garcia-Serres, M. Clémancey, J.-M. Latour, W. Nam, *Angew. Chem. Int. Ed.*, 2014, **53**, 6388; c) B. Wang, Y.-M. Lee, M.S. Seo, W. Nam, *Angew. Chem. Int. Ed.*, 2015, **127**, 11906; d) W.J. Song, Y.J. Sun, S.K. Choi, W. Nam, *Chemistry*, 2006, **12**, 130.

6 A. Lennartson, C.J. McKenzie, *Angew. Chem. Int. Ed.*, 2012, **51**, 6767.

7 a) S.J. Kim, R. Latifi, H.Y. Kang, W. Nam, S.P. de Visser, *Chem. Commun.*, 2009, **96**, 1562; b) Y. Kang, X.-X. Li, K.-B. Cho, W. Sun, C. Xia, W. Nam, Y. Wang, *J. Am. Chem. Soc.*, 2017, **139**, 7444; c) L. Yang, F. Wang, J. Gao, Y. Wang, *Phys. Chem. Chem. Phys.*, 2019, **96**, 1123.

8 a) T. Higuchi, H. Ohtake, M. Hirobe, *Tetrahedron Lett.*, 1989, **30**, 6545; b) H. Ohtake, T. Higuchi, M. Hirobe, *J. Am. Chem. Soc.*, 1992, **114**, 10660; c) Y. Wang, J.H. Espenson, *Org. Lett.*, 2000, **2**, 3525; d) R. Ito, N. Umezawa, T. Higuchi, *J. Am. Chem. Soc.*, 2005, **127**, 834; e) T. Marshall-Roth, S.C. Liebscher, K. Rickert, N.J. Seewald, A.G. Oliver, S.N. Brown, *Chem. Commun.*, 2012, **48**, 7826; f)Y. Wang, L. Zhang, *Synthesis*, 2015, **47**, 289; g) W.-F. Liaw, J.-H. Lee, H.-B. Gau, C.-H. Chen, S.-J. Jung, C.-H. Hung, W.-Y. Chen, C.-H. Hu, G.-H. Lee, *J. Am. Chem. Soc.*, 2002, **124**, 1680; h) K. Nienkemper, V.V. Kotov, G. Kehr, G. Erker, R. Fröhlich, *Eur. J. Inorg. Chem.*, 2006, **2006**, 366.

9 C.-M. Che, J.-S. Huang, *Chem. Commun.*, 2009, 3996.

10 T. Kojima, K. Nakayama, M. Sakaguchi, T. Ogura, K. Ohkubo, S. Fukuzumi, *J. Am. Chem. Soc.*, 2011, **133**, 17901.

11 A. Petrosyan, R. Hauptmann, J. Pospech, *Eur. J. Org. Chem.*, 2018, **2018**, 5237.

12 A. Nielsen, F.B. Larsen, A.D. Bond, C.J. McKenzie, *Angew. Chem. Int. Ed.*, 2006, **45**, 1602.

13 D.P. de Sousa, C. Wegeberg, M.S. Vad, S. Mørup, C. Frandsen, W.A. Donald, C.J. McKenzie, *Chem. Eur. J.*, 2016, **22**, 3810.

14 a) A. Thibon, J.-F. Bartoli, S. Bourcier, F. Banse, *Dalton Trans.*, 2009, **104**, 9587; b)M. Grau, A. Kyriacou, F.C. Martinez, I.M. de Wispelaere, A.J.P. White, G.J.P. Britovsek, *Dalton Trans.*, 2014, **43**, 17108.

15 C. Ducloiset, P. Jouin, E. Paredes, R. Guillot, M. Sircoglou, M. Orio, W. Leibl, A. Aukauloo, *Eur. J. Inorg. Chem.*, 2015, 5405.

16 a) F.T. de Oliveira, A. Chanda, D. Banerjee, X. Shan, S. Mondal, L. Que, E.L. Bominaar, E. Münck, T.J. Collins, *Science*, 2007, **315**, 835; b) M. Ghosh, K.K. Singh, C. Panda, A. Weitz, M.P. Hendrich, T.J. Collins, B.B. Dhar, S. Sen Gupta, *J. Am. Chem. Soc.*, 2014, **136**, 9524.

17 N.T. Vo, Y. Mekmouche, T. Tron, R. Guillot, F. Banse, Z. Halime, M. Sircoglou, W. Leibl, A. Aukauloo, *Angew. Chem. Int. Ed.*, 2019, **58**, 16023.

18 M. Sekino, H. Furutachi, K. Tasaki, T. Ishikawa, S. Mori, S. Fujinami, S. Akine, Y. Sakata, T. Nomura, T. Ogura, T. Kitagawa, M. Suzuki, *Dalton Trans.*, 2016, **45**, 469.

19 We checked that DPPyH can't be oxidized by PhIO w/o catalyst.

20 a) A. Nielsen, F.B. Larsen, A.D. Bond, C.J. McKenzie, *Angew. Chem. Int. Ed.*, 2006, **45**, 1602; b) Y. Liu, S.-M. Ng, S.-M. Yiu, W.W.Y. Lam, X.-G. Wei, K.-C. Lau, T.-C. Lau, *Angew. Chem. Int. Ed.*, 2014, **53**, 14468; c)G. Villar-Acevedo, P. Lugo-Mas, M.N. Blakely, J.A. Rees, A.S. Ganas, E.M. Hanada, W. Kaminsky, J.A. Kovacs, *J. Am. Chem. Soc.*, 2017, **139**, 119; d) E.A. LaPierre, M.L. Clapson, W.E. Piers, L. Maron, D.M. Spasyuk, C. Gendy, *Inorg. Chem.*, 2018, **57**, 495; e) S. Zhan, J.A. De Gracia Triviño, M.S.G. Ahlquist, *J. Am. Chem. Soc.*, 2019, **141**, 10247.

21 S. Kida, J.V. Quagliano, J.A. Walmsley, S.Y. Tyree, *Spectrochim. Acta*, 1963, **19**, 189.

22 J.T. Groves, Y. Watanabe, *J. Am. Chem. Soc.*, 1986, **108**, 7836.

23 C.R. Turlington, P.S. White, M. Brookhart, J.L. Templeton, *J. Organomet. Chem.*, 2015, **792**, 81.

This journal is © The Royal Society of Chemistry 20xx

Please do not adjust margins